Maximum power point tracking CMOS circuit to connect a solar cell into a solid-state battery

L. M. Goncalves, J. F. Ribeiro, J. P. Carmo
MEMS-UMinho R&D Centre
University of Minho, PORTUGAL
{lgoncalves,mgomes,jribeiro,jcarmo}@dei.uminho.pt

***Abstract* — This paper presents a Maximum Power Point Tracking (MPPT) circuit in CMOS technology for integration into an energy harvesting solution, comprising a solid-state thin-film lithium battery fabricated in the back-side of a plastic solar-cell. The MPPT CMOS circuit is required in the energy transfer process from the solar cell to the battery. The MPPT circuit was designed in the 0.7 µm CMOS process from on-semiconductor (former AMIS, Alcatel-Mietec). The pulse width modulation (PWM) gate control of the DC-DC step-up converter is obtained only with analog circuits, which are composed by rail-to-rail operational amplifiers, analog multipliers and a ring oscillator. The ripple correlation control algorithm is used in the implementation of the analog MPPT circuit. This is a dynamically rapid method (e.g., 5 ms step response was measured) where the inevitable ripple of the inductor current of the DC-DC converter is analyzed and used to adjust the set-point of the same DC-DC converter. The full energy harvesting is also described in this paper.**

***Keywords* — Energy harvesting, ripple correlation control, maximum power point tracking.**

I. INTRODUCTION

Harvesting energy from the surrounding environment for self-power/stand-alone electronic circuits has gained increased attention in the last years, either on applications with wireless sensor networks or embedded systems [1,2]. Since surrounding energy source is not always available, a rechargeable battery plays an important role in these systems, enabling a reserve power source and leveling, when the load requires more than the available harvested power. There are different possible energy sources in the environment that can be harvested to power electronic applications [3,4]. The current application uses light energy, however, the concept can be used in almost any energy source with potential for harvesting (for example from mechanical vibrations [5] and thermal gradients [6]). A Maximum Power Point Tracking (MPPT) scheme should be implemented in order to maximize the power transfer from the power source into the rechargeable battery. The reported methods vary in complexity, required sensors, convergence speed, cost, range of effectiveness, implementation hardware, popularity, and so on. The most commonly known MPPT algorithms are hill-climbing, incremental conductance, fractional open-circuit voltage control and perturb and observe, from several others [7]. Most of these techniques are implemented with the help of a digital signal processor control. The Ripple Correlation Control (RCC) is a real-time MPPT method [8] particularly suited for switching power converters because it use the information present in the inherent switching ripple to determine the gradient of the energy-source power-function. Therefore, no additional ripple or perturbation is added to the already present switched converter. That information is available in every switching cycle, enabling a very fast maximum power point tracking [9]. Moreover, the straightforward circuit implementations allow the use of simple analog circuits, easily implemented in a CMOS design. The combination of all of these features makes the RCC distinct from prior methods, and justifies its use in the circuit presented in this paper. Figure 1 illustrates the main blocks of the proposed energy harvesting system. The MPPT controller measures voltage and current in the DC output of energy source and calculates the necessary duty-cycle of the DC-DC converter. The battery charge and protection circuit controls the energy flux between the power source, the battery and the output of the energy harvesting system.

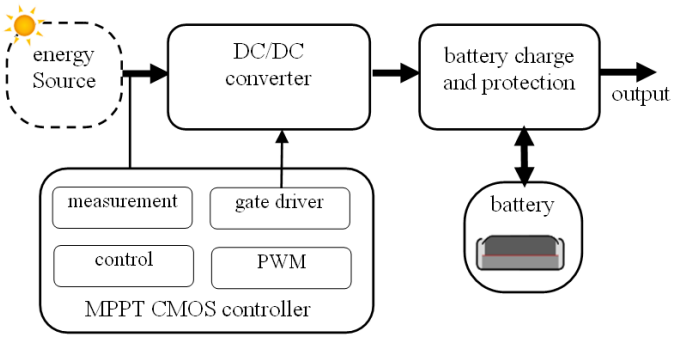

Fig. 1. Functional blocks of the proposed energy harvesting system.

II. ENERGY HARVESTING SYSTEM

A flexible solar cell is used as substrate, where on its back side a solid-state battery of thin-films was previously deposited by Physical Vapor Deposition (PVD), as presented by the authors elsewhere [10]. Previous layers of platinum and titanium were deposited by thermal evaporation (using the technique based on beams of electrons, e-beam) and used as cathode and anode current collectors of the battery, respectively. A cathode of $LiCoO_2$ was deposited by RF-sputtering with 150 W of power source, 40 sccm of argon (Ar) and 300 ºC in the substrate during deposition. The electrolyte LiPON was also deposited by RF-sputtering (150 W of power) in a reactive atmosphere of nitrogen (20 sccm of N_2) from a Li_3PO_4 target. The lithium anode was deposited with 3 µm thickness by thermal

evaporation. Figure 2 presents the materials and a fabricated battery prototype in a polyimide (Kapton© from DuPont) substrate. The two systems are intended to interconnect with the MPPT CMOS circuit and battery charge controller.

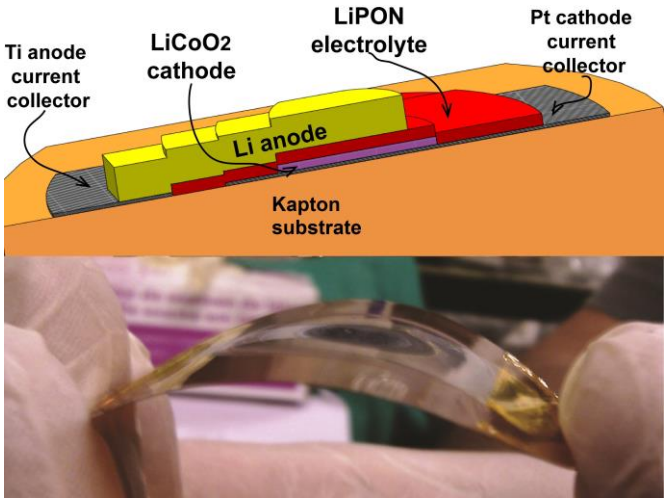

Fig. 2. For the lithium rechargeable solid-state battery: (top figure) an artwork of the proposed materials (not represented at the real scale for a better illustration); and (b) a flexibility demonstration of the fabricated battery on a substrate made of polyimide [10].

III. MAXIMUM POWER POINT TRACKING CONTROLLER

The MPPT controller was based in the RCC method. This method correlates the power of the source variation with the current variation in the inductor of the DC-DC converter. Figure 3 presents a typical boost converter (bottom image) and the IV typical curve of a solar cell (top image). The inset (a) in the top plot of Figure 3 presents the current in the inductor as function of time.

It can be observed that the current that flows through the inductor presents a ripple as a result of the switching frequency. This ripple is represented in the top plot of Figure 3, as a current ripple (ΔI), a voltage ripple (ΔV) and a power ripple (ΔP), in the operating point. In the same figure, a decrease in power is observed (A´-B´) if the current decreases from point A to point B. The MPPT control reacts to this decrease by increasing the duty-cycle of the PWM generator (see Figure 1).

A. Ripple Correlation Control method

Figure 4 presents the functional blocks to implement the RCC algorithm. In this block, the measured voltage value (V) and current value (I) are multiplied in order to compute the power (P). Then, both the power and current derivatives are calculated and also multiplied. The result value (err) is then integrated in order to obtain the PWM (pulse-with-modulator) control voltage ($V_{CONTROL}$). This last voltage represents the set-point of the PWM generator.

B. Low voltage, single supply analog implementation

The complete circuit is presented in Figure 5. A symmetrical supply voltage is necessary to accommodate the results of derivative and multiplier circuits. For this, the input voltage is divided by two (creating a virtual reference in the middle point). The input voltage and current are conditioned by two difference amplifiers. Integrator, derivative, comparator and non-inverter amplifiers circuits are implemented with rail-to-rail operational amplifiers (OpAmp). Figure 6 presents the simulated voltage in the nodes from Figure 5, in the operation point (A-B) in the V/I curve of Figure 3. It can be observed in the simulations that a current decrease corresponds to a power decrease.

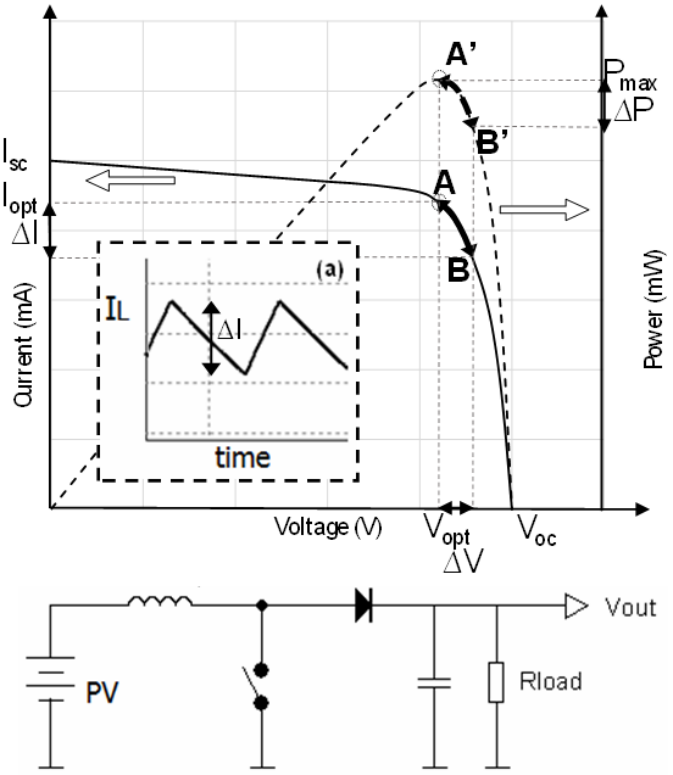

Fig. 3. Boost DC-DC converter and representation of switching ripple in the IV curve of a solar cell. The inset (a) in the top plot highlights the current that flows through the inductor.

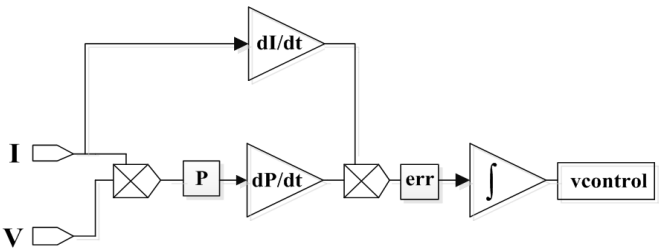

Fig. 4. Block diagram representing the RCC method, where the quantities V and I represent the value of voltage and current in the power source. Additionally, the voltage $V_{CONTROL}$ represents the set-point of the PWM generator.

C. CMOS implementation

The circuits in Figure 5 were designed in the 0.7 µm CMOS on-semiconductor 2-metals/1-poly process (C07-D0.7 µm sub-

technology option) from the on-semiconductor (former AMIS, Alcatel-Mietec foundry) [11].

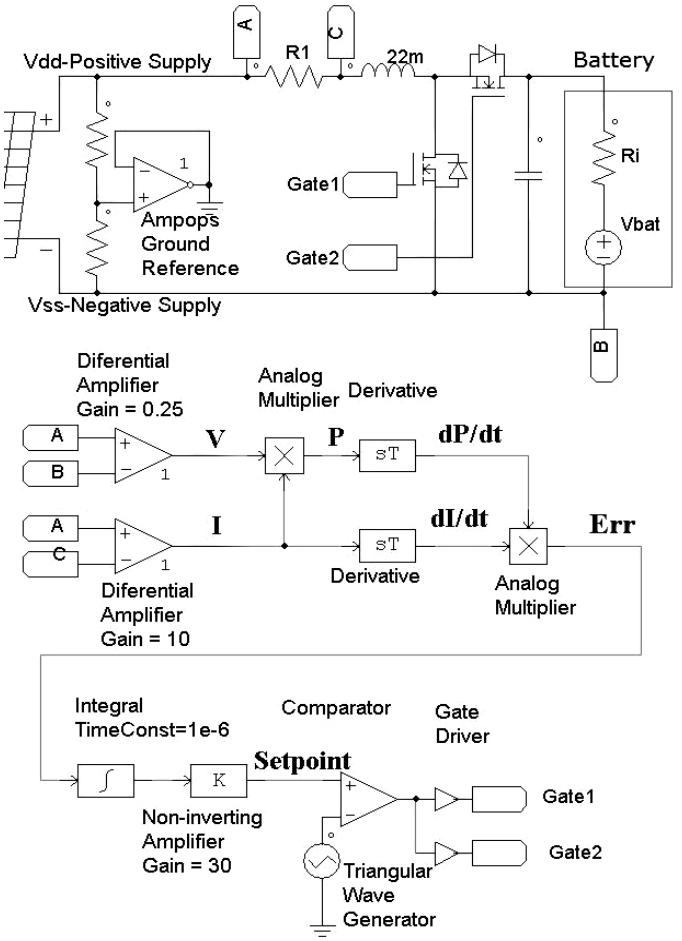

Fig. 5. For the designed CMOS circuit: (on top) the DC-DC boost converter; and (on bottom) the RCC MPPT circuit. Both are represented by functional blocks.

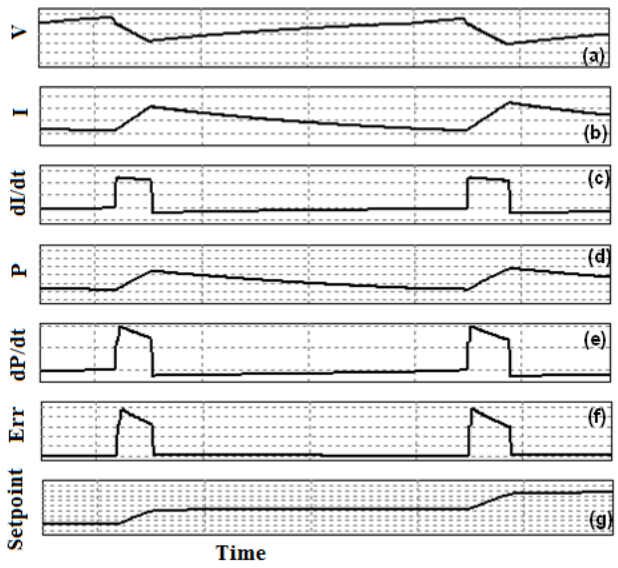

Fig. 6. Simulated voltages, *V*, at the nodes presented in circuit of Figure 5.

Figure 7 shows the rail-to-rail operational amplifier (OpAmp) circuit. The two differential input circuits allow common input voltages bellow and above the supply voltages. The push-pull output allows output voltages up to the rail voltages, with the consequent low output current capability.

The multiplier circuit was implemented using sum-square circuits as presented in Figure 8. This circuit implements the function $V_{O1}=\kappa.(V_1+V_2)^2$. A second circuit was added, with the function $V_{O2}= \kappa.(V_1-V_2)^2$. When the difference of both circuits is considered, $V_O=V_{O1}-V_{O2}=4.\kappa.V_1.V_2$. It is important to note tha the factor κ depends on properties and dimensions of MOSFETs.

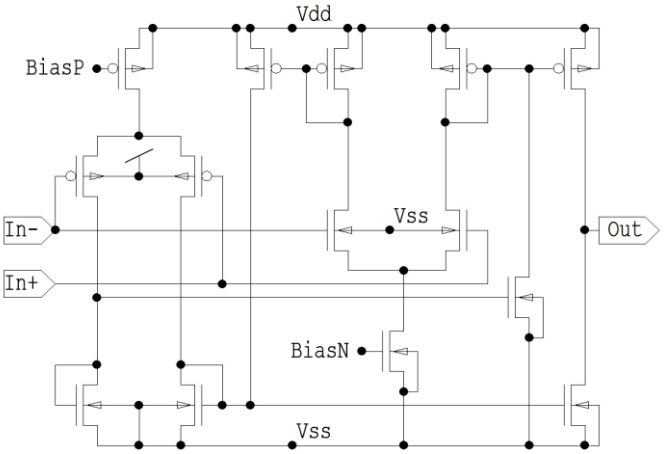

Fig. 7. CMOS rail-to-rail ampop circuit.

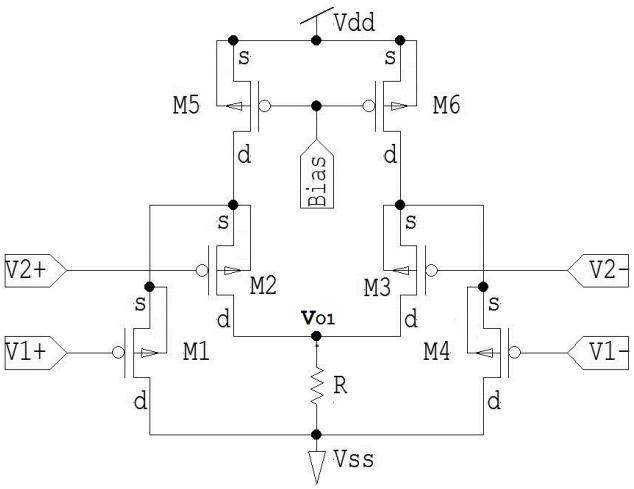

Fig. 8. Sum-square circuit used in the multiplier implementation.

IV. Conclusions

A CMOS circuit to implement the RCC method in MPPT systems was designed and simulated, in the control of a DC-DC boost converter, for low power applications. Only a few external components are needed (resistors, capacitors and inductor). The results demonstrate that the circuit tracks the power source to maximum power in less than 5 ms when a change in source conditions occurs.

ACKNOWLEDGMENTS

This work has been supported by the Portuguese FCT (*Fundação para a Ciência e Tecnologia*) in the scope of the project UID/EEA/04436/2013.

REFERENCES

[1] Chen, L.; Xu, X.; Zeng, P.; Ma, J., "Integration of Energy Harvester for Self-Powered Wireless Sensor Network Nodes", International Journal of Distributed Sensor Networks, Vol. 2014, pp. 1-7, #782710..

[2] Liu, Z.; Yang, X.; Yang, S.; McCann, J., "Efficiency-Aware: Maximizing Energy Utilization for Sensor Nodes Using Photovoltaic-Supercapacitor Energy Systems", International Journal of Distributed Sensor Networks, Vol. 2013, pp. 1 11, #627963.

[3] Harb, Adnan. "Energy harvesting: State-of-the-art." Renewable Energy 36.10 (2011): 2641-2654.

[4] Morais, Raul, et al. "Sun, wind and water flow as energy supply for small stationary data acquisition platforms." Computers and electronics in agriculture 64.2 (2008): 120-132.

[5] Rocha, J.G.; Goncalves, L.M.; Rocha, P.F.; Silva, M.P.; Lanceros-Mendez, S., "Energy harvesting from piezoelectric materials fully integrated in footwear", IEEE Transactions on Industrial Electronics, Vol. 57, No. 3, pp. 813-819, March 2010

[6] Maharaj, S.; Govender, P., "Waste energy harvesting with a thermoelectric generator," Domestic Use of Energy Conference (DUE), 2013 Proceedings of the 21st , vol., no., pp.1,6, 3-4 April 2013

[7] Esram, Trishan, and Patrick L. Chapman. "Comparison of photovoltaic array maximum power point tracking techniques." IEEE Transactions on Energy Conversion EC 22.2 (2007): 439.

[8] Kimball, Jonathan W., and Philip T. Krein. "Discrete-time ripple correlation control for maximum power point tracking." Power Electronics, IEEE Transactions on 23.5 (2008): 2353-2362.

[9] Esram, Trishan, et al. "Dynamic maximum power point tracking of photovoltaic arrays using ripple correlation control." Power Electronics, IEEE Transactions on 21.5 (2006): 1282-1291.

[10] Ribeiro, J. F., et al. "Flexible thin-film rechargeable lithium battery.", 2013: The 17th International Conference on Transducers & Eurosensors XXVII. IEEE, 2013.

[11] Europractice IC Service: low-cost ASIC prototyping (MPW) and small-medium volume production, 0.7 µm CMOS on-semiconductor (formerly AMI Semiconductor) 2-metals/1-poly process, C07-D0.7 µm option. **www.europractice-ic.com/technologies_AMIS_tech.php**.